PCCP

Accepted Manuscript




ROYAL SOCIETY OF CHEMISTRY

www.rsc.org/pccp

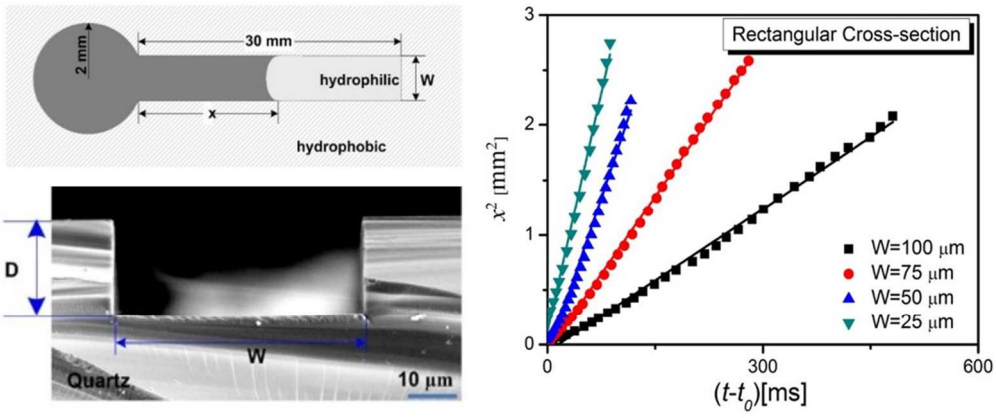


For capillary-driven liquid-liquid displacement in rectangular open microchannels, the square of the position of the liquid-liquid front increases linearly with time, whereas the flow velocity decreases with increasing channel width.
210x89mm (150 x 150 DPI)

Journal Name

RSCPublishing

ARTICLE

# Dynamics of Capillary-Driven Liquid-Liquid Displacement in Open Microchannels

Cite this: DOI: 10.1039/x0xx00000x

D. Yang,[a,b] M. Krasowska,[a] C. Priest[a] and J. Ralston[*,a]

Received 00th January 2012,
Accepted 00th January 2012

DOI: 10.1039/x0xx00000x

www.rsc.org/

The dynamics of the spontaneous spreading of a liquid droplet along an open hydrophilic microchannel filled with another immiscible liquid, is primarily determined by the competition between the capillary driving force and the viscous drag. While the former force depends on the channel cross-section and dimensions, interfacial tension between two liquids and the contact angle formed between the channel's wall and the two liquids, the latter arises from the motion of fluid molecules in the two bulk liquids. This paper focuses on to the influence of the outer (displaced) phase viscosity. In general, as the viscosity of the displaced phase increases relative to the viscosity of the displacing phase, the velocity of the liquid-liquid meniscus decreases. The experiments were interpreted by extending a previously established correlation for liquid-vapour systems (J. Phys. Chem. C, 2011, 115 (38), 18761-18769) in open microchannels of the same geometry. The relationship between the liquid-liquid flow dynamics and the properties of the liquids (e.g. viscosities) is still unclear. Nonetheless, by taking a self-consistent empirical approach to estimate the influence of the viscosities on the flow kinetics for a given system, it is possible to obtain a reasonable theoretical description for the experimental system over a specific range of viscosity ratios.

Keywords: Capillary flow; Microfluidics; Washburn; liquid-liquid displacement;

## Introduction

'Open' microchannels are straight-forward to fabricate, simple to clean, and surface modification can be achieved using existing methodologies, which offers significant potential for use in microfluidic devices. The risk of channel clogging from ambient materials is off-set by the ease with which the channels can be cleaned for use and, in some cases, re-use. On the other hand, the flow in open channels cannot be driven by positive pressures applied to a reservoir of fluid, i.e. via traditional high-precision pumps, because the fluid can escape through the open side of the channel. Alternative approaches to achieving flow include non-mechanical pumping mechanisms: interfacial tension-driven capillary action[1, 2], thermocapillary[3, 4] and electrowetting[5, 6]. These techniques exploit the advantage of the high surface-to-volume ratios involved to drive the fluid. Capillary-driven flow has the additional advantage that no additional equipment, such as power supplies, are required, making it ideal for handheld and disposable devices for diagnostic applications on-site, especially in remote locations.

Capillary-driven flow refers to the spontaneous penetration of a liquid into a confinement – usually a channel or pore (e.g., a capillary tube, porous soil, or paper) - to displace a second fluid. The process is driven by the Laplace pressure across the curved meniscus and, for a cylindrical confining geometry, the rate of liquid penetration (against its vapour phase) has been successfully described by Washburn[7]:

$$x^2 = \frac{\gamma R \cos\theta}{2\mu} t \quad (1)$$

Where $x$ is the distance to the meniscus from the entrance of the capillary, $R$ is the radius of the cylindrical capillary, $\mu$ is the dynamic viscosity of the liquid phase, $\gamma$ is the interfacial tension of the liquid, $\theta$ is the static contact angle of the liquid on the channel wall, and $t$ is time. Eq. (1) predicts a linear dependence of $x^2$ with time $t$, which can be simplified to:

$$x^2 = k \times t \quad (2)$$

where $k$ is a 'mobility parameter' that depends on the details of the particular system (the channel dimensions, liquid properties, and wall wettability).

In microfluidic applications, the channel geometry is not often a cylinder and one might expect that other common geometries will play a key role in dictating the performance of the device. We have previously shown that for wet (HF) and dry (plasma) etched open microchannels in glass, which has a very different flow field (due to a free and deformable interface present), the linear dependence of $x^2$ on $t$ holds[8]. The same dependence was also observed for open channels with different geometries, including triangular[2, 9], rectangular[10], and skewed U-shaped[10] channels. In our previous study, we also observed that the meniscus velocity decreased with increasing channel width[8], which, at first glance, appears to counter Washburn's prediction of faster meniscus velocities for increasing capillary radii. There is no contradiction, however, since the width and height of the channel must both be considered, as discussed below.

The similarity in the dynamics observed for capillaries and open channels led us to calculate the mobility parameter, $k$, used in Eq. (2). It was assumed that the flow is driven by the change in the free energy of the system as the liquid advances along the channel, and is opposed by the hydrodynamic viscous friction. After the initial transient regime (as the liquid accelerates near the entrance of the channel), these two forces balance one another. The result of this force balance, which is derived elsewhere[8], indeed predicts a linear dependence as observed in our experiments, with the mobility parameter given by the equations:

$$k = \frac{2\gamma D}{\mu}\frac{[2\cos\theta-(1-\cos\theta)p]}{p^2}g(p) \quad (3)$$

with

$$\begin{cases} g(p) = \frac{16}{\pi^5}\sum_{n\geq 0,n\ odd}\frac{1}{n^5}\left[\frac{n\pi}{2}p - \tanh\left(\frac{n\pi}{2}p\right)\right] \text{ (no-slip BC)} \\ g(p) = \frac{128}{\pi^5}\sum_{n\geq 0,n\ odd}\frac{1}{n^5}\left[\frac{n\pi}{4}p - \tanh\left(\frac{n\pi}{4}p\right)\right] \text{ (full-slip BC)} \end{cases} \quad (4)$$

In Eqs. (3) and (4), $p=W/D$ denotes the aspect ratio of the channel width $W$ to the depth $D$, while the function $g(p)$ describes the dependence of the average flow velocity, thus of the viscous friction, on the aspect ratio of the cross section of the channel (rectangular channels). The increased width of the channel leads to an increase in both the capillary driving force and the viscous resistance, while the latter is increased more than the capillary force. Thus a faster velocity was observed in narrower channels.

Liquid displacement of vapour in microchannels is an important phenomenon, particularly upon first-fill of a chip. However, liquid-liquid displacement is also very relevant to microfluidic systems and is of great importance in many industrial processes, including enhanced oil recovery and lubrication[11, 12]. The obvious difference from the more commonly studied liquid-vapour displacement lies in the fact that the viscosity of the outer (displaced) phase is seldom negligible compared to that of the inner (displacing) phase. Among the few liquid-liquid systems investigated[13-17], most have focused on liquid flow in closed channels, usually in circular capillaries. An analogous Washburn approach has been used to derive the dynamics of liquid-liquid flow in closed channels. However discrepancies between theoretical predictions and the experimental results have been observed. Although these discrepancies are usually attributed to the excess energy dissipation at the three phase contact line[13, 16] a definite answer is yet to be obtained. In spite of its relevance, a complete description of the kinetics of liquid-liquid displacement in capillaries (or other closed or open geometries) is still lacking. Note that, for all of the studies of liquid-liquid displacement in capillaries, the hydrodynamic contributions of the displaced fluid were neglected, based on the assumption that the viscosity of the displaced liquid is not important for the flow kinetics. The effect of the displaced phase viscosity when it is comparable to the viscosity of the displacing phase on the dynamics of capillary-driven flow is still an open question.

In this study, we have continued our investigation of the physical and material parameters which influence the dynamic of wetting in open microchannels[8] by investigating the flow dynamics of one liquid displacing another immiscible liquid. For spontaneous spreading, the dynamics of the liquid spreading along a channel is primarily determined by the competition between the capillary driving force and the viscous drag force arising from the fluid motion in the two bulk liquids. Similarly to the previous studies of liquid-liquid displacement on a flat surface,[18, 19] the aim here is to establish the role played by the viscosities of the two liquids and their interfacial tension on the dynamics of the liquid-liquid displacement in an open microchannel.

## Experimental

### Materials

1-undecanethiol (98%), octanol (99%), decyl alcohol (99%), dodecane (99%), tetradecane (99%) and hexadecane (99%) were purchased from Sigma-Aldrich and used in the present study without further purification. Ethanol (A.R., 99%), propan-2-ol (A.R.), and glycerol (99.5%) were obtained from Chem-Supply, Australia. Toluene (99.8%) was supplied by Merck Pty Ltd. Ultrapure water with a pH of 5.6 ± 0.1, a resistivity of 18.2 MΩ•cm and interfacial tension 72.4 mN/m at 22 °C, was obtained from a NANOpore Diamond Barnstead system, and used in all experiments.

### Sample preparation and characterization

The microchips were prepared according to a procedure described previously using the same materials[8]. The channel widths range from 25 µm to 100 µm with a depth of 19.1 µm. The schematic diagram of the channel is presented in Figure



 

1A. Scanning electron microscopy (SEM) was used to image the cross section of the channels (see Figure 1B). SEM images confirmed the channel shape. The etched channels were uniform and smooth, ideal for this experimental study.

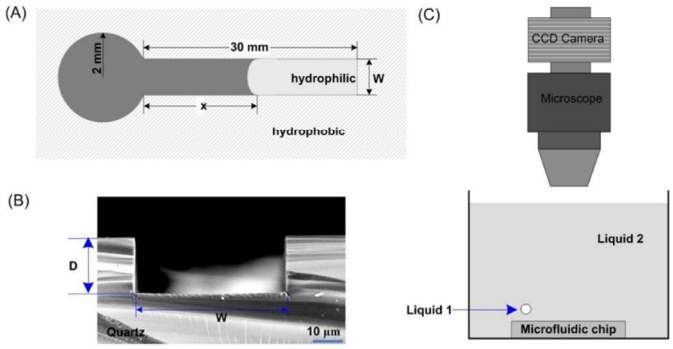


**Figure 1.** (A) Schematic diagram of liquid flow from a reservoir into a hydrophilic microchannel of width *W*. The liquid reservoir is a circular indentation (depth equal to that of the channel) with a diameter of 4 mm. (B) SEM micrograph of the cross-section of the rectangular channel showing width *W*, depth *D*. (C) Experimental arrangement for dynamic top-view measurements.

### Experimental set-up

The experimental set-up is shown in Figure 1C. A high speed camera (Photron, 1024 PCI) mounted on a microscope (Olympus, U-AN360-3) with 10x objective magnification was used for the experiments of liquid flow in open microchannels. The sample was placed in a clean glass Petri dish and immersed in a second liquid phase (organic phase), and a 5 µL MilliQ water (or MilliQ water/glycerol mixture) droplet was deposited, with a syringe pump (Cole Parmer), onto the reservoir area. Once the droplet contacted the inlet of the channel, the liquid started flowing in the microchannel due to the capillary force. The high speed camera (collecting frames with frequency of 2000 Hz) allowed the position of the meniscus as a function of time to be tracked. The field of view for a single measurement is approximately 0.9 x 1.8 $mm^2$. The software used for a graphic analysis of the recorded frames was ImageJ®. After each experiment, the sample was rinsed thoroughly with ethanol and MilliQ water and stored in a closed glass container under MilliQ water for further use. For each channel and liquid-liquid combination, three series of independent measurements were conducted, showing good agreement between experiments.

## Results and Discussion

Individual drops of liquid 1 were dispensed from a gas-tight micro syringe (Hamilton), and allowed to approach, under the influence of gravity, the reservoir of the channel (the reservoir, the channel, and the drop are all immersed in the immiscible liquid 2). The liquid 1 is chosen such that it wets the substrate better than liquid 2. After arriving at the liquid 2-solid interface, the drop spreads and gradually fills the surface of the reservoir. Once liquid 1 spreads to meet the inlet of the channel, it begins to fill the hydrophilic channel due to the capillary force. Measurement of the motion of the liquid-liquid meniscus began from the inlet of the channel. A typical plot of the distance of the moving meniscus, *x*, against time, t, is shown in Figure 2 for the dynamic liquid-liquid displacement in rectangular channels for four different channel widths.

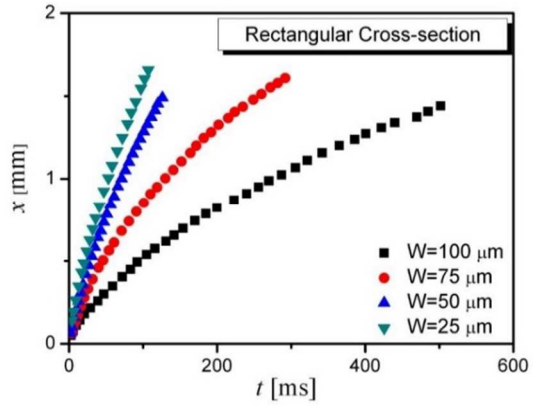


**Figure 2.** The progress of the liquid meniscus, *x*, versus time, *t*, for pure water displacing hexadecane (HD) in rectangular open channels of different width.

In comparison with liquid-vapour systems in the previous study[8], the dynamics for liquid-liquid systems is significantly slower, often by at least one order of magnitude. However, the qualitative behaviour is the same in both cases; the motion of the meniscus is always faster in a narrower microchannel. In Figure 3, the squared position of the meniscus, $x^2$, is plotted against time, *t*, for water displacing hexadecane in rectangular cross-section microchannels. A linear relationship between the two is observed (this was also observed for all other liquid-liquid systems examined in this study as listed in Table 1). In a similar manner to liquid-vapour systems, the linearity starts only after a short time $t_0$ ($t_0$ was determined by taking the intercept of the time axis based on a linear fit to the experimental data to an $R^2$ value > 0.9996, achieved by progressively excluding the earliest data points in the linear fit), as shown in Figure 3. Typical values for $t_0$ are within 0.02 s for liquid-liquid displacement in rectangular microchannels (for channel widths of 15, 25, 50, 75 µm, $t_0$ was 21, 12, 10, 20 ms, respectively). As the moving meniscus is followed for at least several hundreds of milliseconds, a regime of linear dependence of $x^2$ with *t* appears to be well-established.

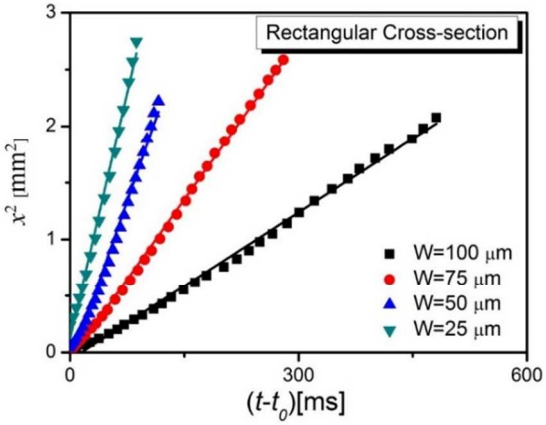


**Figure 3**. The progress of the liquid meniscus, $x^2$, with time, $t$-$t_0$, for pure water flowing against hexadecane in rectangular microchannels. The solid lines show the linear fit, $x^2=k(t-t_0)$ , to the data in the linear regime.

**Table 1** Liquid-liquid systems and their material properties (T = 22 ± 1°C) [a]

| System[b] | $\mu_1$ (mPa·s) | $\mu_2$ (mPa·s) | $\lambda(\mu_2/\mu_1)$ | $\gamma_{12}$ (mN/m) |
|---|---|---|---|---|
| 30% glycerol-water /toluene | 2.98 | 0.52 | 0.17 | 29.8 |
| 20% glycerol-water /toluene | 1.99 | 0.52 | 0.26 | 30.8 |
| 30% glycerol-water /dodecane (DD) | 2.98 | 1.30 | 0.44 | 41.1 |
| 20% glycerol-water /dodecane | 1.99 | 1.30 | 0.65 | 42.8 |
| Water/dodecane | 0.89 | 1.30 | 1.46 | 50.5 |
| Water/tetradecane (TD) | 0.89 | 2.09 | 2.35 | 51.1 |
| Water/hexadecane (HD) | 0.89 | 3.16 | 3.55 | 51.3 |
| Water/octanol (OC) | 0.89 | 7.94 | 8.92 | 8.5 |
| Water/decanol (DC) | 0.89 | 12.45 | 13.99 | 8.5 |

[a] The index 1 is used for displacing phase, while index 2 is used for the displaced phase.
[b] The percentage refers to the volume percentage

Increasing the viscosity $\mu$ of the liquids slows down the velocity of the meniscus but does not affect the linear dependence noted above nor the dependence of the rate of spreading on the width of the channel. In summary, for all of the liquid-liquid systems studied (listed in Table 1) after a transient time $t_0$, the flow dynamics obeys the same linear dependence given by Eq. (2) but with a different mobility parameter, *k'*:

$$x^2 \approx k' \times t \quad (5)$$

(Note that *k* and *k'* are essentially the same and *k'* was used for a distinction between liquid-liquid and liquid-vapour systems). Similar to *k*, *k'* depends on the details of the particular system (including the channel cross-section and dimensions, and the viscosity and interfacial tension of the liquids). Deriving the expression for the mobility parameter *k'*, is a very difficult task because of the need to compute the velocity profile for a two-phase flow in such open geometry.

The key factor for liquid-liquid displacement is the viscosity ratio of the displaced phase to the displacing phase, $\lambda$. The fact is that a relationship between the velocity of the moving meniscus and the properties of the liquids (e.g., viscosities and interfacial tension) for liquid-liquid displacement in microchannels is still not clear. However, it may be expected that, at least qualitatively, the dynamics for liquid-vapour systems would be similar to that of liquid-liquid systems where the viscosity of the spreading phase is much greater than that of the displaced phase[20], and that a transition to this would be observed as the viscosity ratio approached zero. For non-zero values of this ratio, it is expected that the two viscosities enter explicitly into the expression for the flow dynamics. An empirical derivation of this dependency, which is based on an extension of the approach used for the case of the liquid-vapour system[8], is developed below.

In all of the liquid-liquid systems investigated, for a given displacing liquid, the displacement rate decreases as the viscosity of the displaced phase increases. When the mobility parameter, *k'* in Eq. (5) is plotted against the aspect ratio, *p* (*p* = *W/D*), the data correlation between *k'* and *p* for each system retains the general shape of the liquid-vapour correlation, but is shifted to lower values of *k'* with increasing viscosity ratio, $\lambda$ (see Fig. 4).

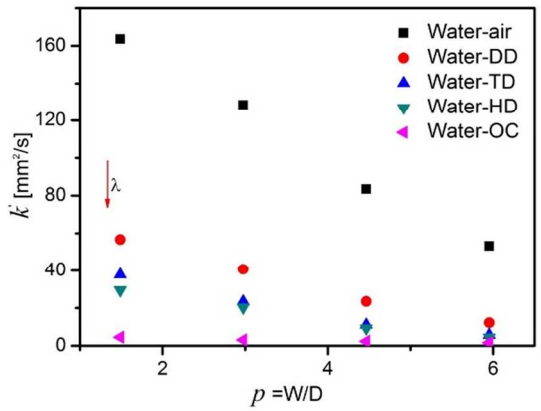


**Figure 4.** Experimental derived mobility parameter values, *k'* (derived from Eq. (5)), for water flow against another liquid phase in different rectangular channels with various aspect ratios, *p*.

Obviously, the dependence of the flow velocity on the viscosity of the displaced phase is not negligible. This is in agreement with the hydrodynamic investigation of droplet spreading on a flat surface surrounded by another immiscible liquid by Foister[18], who performed experiments over a wide range of viscosities.

Thus, a simple vertical shift factor, α, was determined for each system such that the data could be collapsed onto the correlation for the liquid-vapour system. α was defined as:

$$k' = \alpha k \quad (6)$$

Where *k* is the mobility parameter describing the dynamics of liquid-vapour displacement in open rectangular channel, see Eq. (3)[8].

Eq. (3) fits the results remarkably well with a no-slip boundary condition at the liquid-vapour interface. A similar immobile boundary condition may also apply at a liquid-liquid interface[21-23] and was assumed that this is the case for the liquid-liquid displacement experiments here. In Eq. (3), it is noted that the mobility parameter, *k*, for water displacing vapour, consists of a

dimensional factor involving some physical parameters (e.g. interfacial tension and viscosity) and a scalar, function *g(p)* which dictates the exact shape (the 'master curve'). For the same liquid-liquid displacement in the same channel, the reason for *k'* to vary when vapour is replaced by another liquid is solely that the liquid properties (e.g. interfacial tension and viscosity) change, corresponding to the change of driving force and viscous drag force. The influence of the change in the driving force may be calculated using a surface energy analysis[2, 8] as has been discussed in the previous study[8]. If it is assumed that the contact angle is small and that the displacing liquid completely fills the channel, the influence from the change of the interfacial tension to the mobility parameter *k'* can be written as:

$$k' \sim \frac{\gamma_{12}}{\gamma_1} k \tag{7}$$

The influence of the change of the viscous drag force remains unclear. Here, it is assumed that the effect of the displaced phase viscosity can be accounted by a function, $\alpha(\lambda)$, depending only on the viscosity ratio $\lambda$, not on each of the viscosities independently. According to this assumption, Eq. (7) can be written as:

$$k' = \frac{\gamma_{12}}{\gamma_1} \alpha(\lambda) k \tag{8}$$

For each set of data, $\alpha(\lambda)$, can be calculated from the experimentally derived values, $\alpha$ , and the ratio of the interfacial tensions. The values $\alpha(\lambda)$ are listed in Table 2.

**Table 2.** Shift factors for the correlation of liquid-liquid with liquid-vapour systems.

| System | $\lambda$ | $\alpha$ | $\alpha(\lambda)$ |
|---|---|---|---|
| Water/DD | 1.46 | 0.30 | 0.43 |
| Water/TD | 2.35 | 0.18 | 0.25 |
| Water/HD | 3.55 | 0.15 | 0.21 |
| Water/OC | 8.92 | 0.023 | 0.18 |
| Water/DC | 13.99 | 0.015 | 0.13 |

A power law fit to this finite set of values, is proposed in this

$$\alpha(\lambda) = x(1+\lambda)^y \tag{9}$$

study. As shown in Figure 5, this model is compatible with the experimental results; the fitting parameter obtained are $x=1$ and $y=-1$, with a correlation coefficient $R^2$ of 0.9.

The proposed dependence of $\alpha(\lambda)$ on $\lambda$ is particularly simple and physically reasonable in that the viscous dissipation arising from the fluid flow in the two bulk liquids enters simply as a

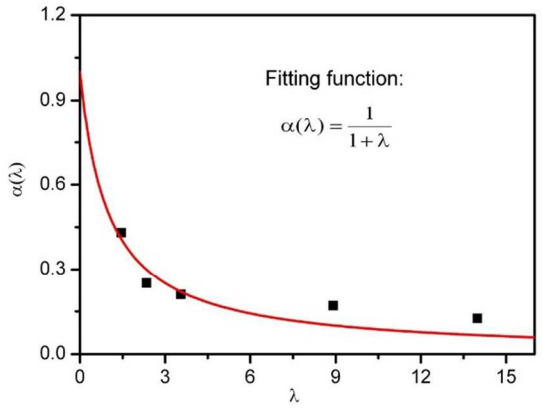


**Figure 5**. Derived $\alpha(\lambda)$ values versus viscosity ratio, $\lambda$. Line corresponds to the best fit of the data ($R^2$=0.9).

sum of viscosity terms. Also, it has the correct asymptotic limits, i.e., so that in the limit of either $\lambda >> 1$ or $\lambda << 1$, the flow dynamics becomes that of the displacing, or being displaced by air. If Eq. (9) holds, Eq. (8) can then be expressed as:

$$k' \approx \frac{1}{1+\lambda} \frac{\gamma_{12}}{\gamma_1} k \tag{10}$$

Eq. (10) is then rewritten as:

$$k' \approx \frac{2\gamma_{12} D}{\mu_1+\mu_2} \frac{[2\cos\theta - (1-\cos\theta)p]}{p^2} g(p) \tag{11}$$

This velocity dependence on the sum of viscosities with comparable viscosity ratio was also observed for liquid-liquid displacement on a flat surface[18, 19]. This empirical prediction for the flow dynamics will now be considered against the experimental data obtained for other liquid-liquid systems, such as water-glycerol mixtures displacing a variety of liquids, as described below.

Eq. (11) predicts that for fixed *D* (which is the case of the present study), the product $[(\mu_1+\mu_2)/\gamma_{12}]k'$ is a function of the aspect ratio *p* only. Figure 6 showed that, when plotted in this way, there is a good collapse of the experimental data onto a master curve. This compares well with the prediction of Eq. (11), which implicitly assumed a no-slip boundary condition at the liquid-liquid interface.

In our previous work[8], it was noted that, liquid 'fingers' were observed extending ahead of the meniscus along the sides of the channels with larger aspect ratios for liquid displacing air in open microchannels. However, it turned out that this liquid morphology change has only relatively minor effects. A similar phenomenon was also observed for liquid-liquid displacement in open rectangular microchannels in wider channels (*W/D* from 3.9 to 5.4); the effects are small in this case, too, judging

from the fact that the empirical predictions are close to the experimental data obtained by using the meniscus base as the reference for monitoring liquid motion (Fig. 6). It should also be noted that the empirical model proposed here is only valid if there exists no instability at the advancing meniscus front that leads to viscous fingering.

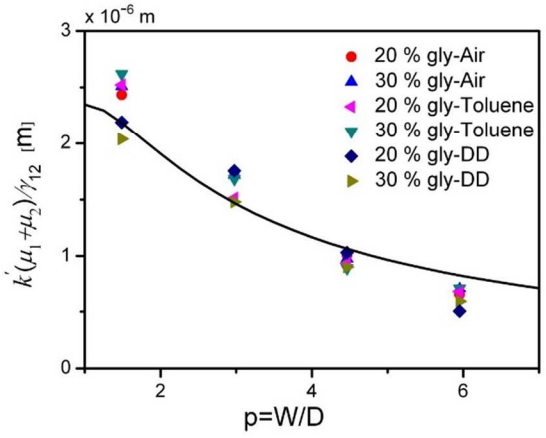


**Figure 6.** Comparison between the product $[(\mu_1+\mu_2)/\gamma_{12}]k'$ calculated from Eq. (11), solid line and the values obtained from fitting out experimental data, symbols, for channel of various aspect ratios, *p*.

## Conclusions

Capillary-driven liquid-liquid displacement, where a drop of one liquid spreads against another immiscible liquid along an open microchannel, has been investigated experimentally. The results show that the square of the position of the liquid front (with respect to the inlet of the channel) increases linearly with time. The flow velocity decreases with increasing channel width, in a similar manner to liquid-vapour systems. As the viscosity of the external (displaced) phase increases relative to the viscosity of the displacing phase, the velocity of the liquid front decreases. An empirical formula describing the influence of the viscosities and of the liquid-liquid interfacial tension on the dynamics of immiscible liquid-liquid displacement was developed and successfully tested for systems within a significant range of viscosity ratios.

## Acknowledgements

Discussions with Dr. Mihail N. Popescu are warmly acknowledged. Photolithography masks were printed at Optofab, Australia. Microfluidic channels were prepared at the South Australian node of the Australian National Fabrication Facility, a company established under the National Collaborative Research Infrastructure Strategy to provide nano and micro-fabrication facilities for Australia's researchers. The authors acknowledge the financial support from the Australian Research Council Linkage and Discovery Project schemes, grants AMSRI and DP1094337.

## Notes and references

[a] Ian Wark Research Institute, University of South Australia, Mawson Lakes SA 5095, Australia.
[b] Centre for Environmental Risk Assessment and Remediation, University of South Australia, Mawson Lakes, SA 5095, Australia.
* Corresponding author. Phone: + 61 (0)8 8302 3066; Fax: + 61 (0)8 8302 3683; e-mail address: john.ralston@unisa.edu.au

1. A. A. Darhuber, S. M. Troian and W. W. Reisner, *Phys. Rev. E: Stat.Nonlin. Soft Matter Phys.*, 2001, **64**, 031603/031601.
2. R. R. Rye, J. A. Mann and F. G. Yost, *Langmuir*, 1996, **12**, 555.
3. A. A. Darhuber, J. M. Davis, S. M. Troian and W. W. Reisner, *Phys. Fluids*, 2003, **15**, 1295.
4. D. E. Kataoka and S. M. Trolan, *Nature*, 1999, **402**, 794.
5. J.-C. Baret, M. Decre, S. Herminghaus and R. Seemann, *Langmuir*, 2005, **21**, 12218.
6. J.-C. Baret, M. M. J. Decre, S. Herminghaus and R. Seemann, *Langmuir* 2007, **23**, 5200.
7. E. W. Washburn, *Phys. Rev.* , 1921, **17**, 273.
8. D. Yang, M. Krasowska, C. Priest, M. N. Popescu and J. Ralston, *J. Phys. Chem. C*, 2011, **115**, 18761.
9. R. R. Rye, F. G. Yost and J. A. Mann, *Langmuir*, 1996, **12**, 4625.
10. Y. Chen, L. S. Melvin, S. Rodriguez, D. Bell and M. M. Weislogel, *Microelectron. Eng.*, 2009, **86**, 1317.
11. D. F. Leclerc and G. H. Neale, *J. Phys. A: Math. Gen.* , 1988, **21**, 2979.
12. J. Silver, Z. Mi, K. Takamoto, P. Bungay, J. Brown and A. Powell, *J Colloid Interface Sci*, 1999, **219**, 81.
13. T. E. Mumley, C. J. Radke and M. C. Williams, *J Colloid Interface Sci*, 1986, **109**, 398.
14. T. E. Mumley, C. J. Radke and M. C. Williams, *J Colloid Interface Sci*, 1986, **109**, 413.
15. M. Fermigier and P. Jenffer, *J. Colloid Interface Sci.*, 1991, **146**, 226.
16. P. Van Remoortere and P. Joos, *J. Colloid Interface Sci.*, 1993, **160**, 397.
17. W. K. Chan and C. Yang, *J. Micromech. Microeng.*, 2005, **15**, 1722.
18. R. T. Foister, *J Colloid Interface Sci* 1990, **136**, 266.
19. M. Ramiasa, J. Ralston, R. Fetzer and R. Sedev, *J. Phys. Chem. C* 2011, **115**, 24975.
20. S. Basu, K. Nandakumar and J. H. Masliyah, *J Colloid Interface Sci*, 1996, **182**, 82.
21. R. Manica, J. N. Connor, S. L. Carnie, R. G. Horn and D. Y. C. Chan, *Langmuir*, 2006, **23**, 626.
22. J. N. Connor and R. G. Horn, *Farad. Discuss.*, 2003, **123**, 193.
23. E. Klaseboer, J. P. Chevaillier, C. Gourdon and O. Masbernat, *J. Colloid Interface Sci.*, 2000, **229**, 274.